

Effect of Heating on the Constitution of Na⁺- and CO₃²⁻-Containing Apatites Obtained by the Hydrolysis of Monetite

Erna A. P. De Maeyer, Ronald M. H. Verbeeck,*¹ and Didier E. Naessens

Laboratory for Analytical Chemistry, University of Ghent, Krijgslaan 281-S12, B-9000 Ghent, Belgium

Received June 3, 1994[®]

This study investigates the heating process of Na⁺- and CO₃²⁻-containing apatites obtained by the hydrolysis of monetite. The results of the chemical and physical analyses of the samples reveal that all the water was removed after heating at 400 °C. Moreover, no other drastic constitutional changes take place. On this basis, the exact unit cell composition of these apatites could be calculated. From this composition, it was deduced that, apart from the two predominant mechanisms [Ca²⁺ + PO₄³⁻ + OH⁻ ↔ V^{Ca} + CO₃²⁻ + V^{OH}] and [Ca²⁺ + PO₄³⁻ ↔ Na⁺ + CO₃²⁻], a small part of the Na⁺-ions is incorporated in the apatite lattice independently of CO₃²⁻ according to the mechanism [Ca²⁺ + OH⁻ ↔ Na⁺ + V^{OH}] with V^X representing a vacancy on a regular apatite lattice site occupied by X. The dependency of the contributions of these mechanisms on the Na₂CO₃ concentration in the hydrolysis solution differs, suggesting that the mechanisms are not completely coupled.

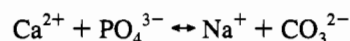
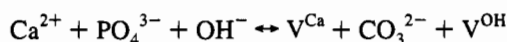
Introduction

Calcium hydroxyapatite, Ca₁₀(PO₄)₆(OH)₂ (HAp), is generally considered as the prototype for the mineral phase of the calcified tissues of higher vertebrates.² However, in these biominerals as well as in mineral apatites such as francolite, part of the lattice ions of HAp is substituted by other ions, especially CO₃²⁻ and Na⁺. In this respect, these minerals should be considered rather as substitutional solid solutions. Such substitutions have considerable influence on the physical, chemical and physico-chemical properties of the solid and, consequently, on the mineralization, demineralization and remineralization processes of the calcified tissues. In order to derive the fundamental thermodynamic properties of the solid which determine the course of these processes, the mechanisms by which CO₃²⁻ and Na⁺ are incorporated into the apatite lattice, must be known. Since the biological apatites are too complex, e.g. they are associated with an organic phase and they contain an appreciable number of trace elements,² such a study should be performed using synthetic samples.

In a previous study,³ Na⁺- and CO₃²⁻-containing apatites (NCAp's) were prepared by the hydrolysis of monetite, CaHPO₄, in Na₂CO₃ solutions at 95 °C. A suitable choice of reaction parameters could guarantee the preparation of single phase, uncontaminated NCAp's containing no HPO₄²⁻ ions, under homogeneous precipitation conditions.⁴ This is in opposition to the heterogeneous precipitation methods often used in the past⁵⁻⁹ which are hardly controllable.³

The NCAp's were thoroughly analysed chemically as well as physically.³ From the relative composition and the results of the physical analysis, it was found that the samples were

apatites containing CO₃²⁻ on PO₄³⁻ lattice sites (i.e. so called B-type CO₃²⁻). Moreover, the results suggested that the predominant substitution mechanisms responsible for the incorporation of Na⁺ and CO₃²⁻ in these apatites correspond to



where V^X stands for a vacancy on a regular apatite lattice site occupied by X. However, the precipitates still contained an appreciable amount of water even after prolonged drying under vacuum at 25 °C. Consequently, the content of the apatite unit cell could not be derived and hence the exact absolute contribution of these mechanisms to the stoichiometry of NCAp could not be deduced. Higher drying temperatures are probably required to remove the water. However, such a heating process should be carried out with great care, since some studies suggest that severe constitutional changes, especially a loss of CO₃²⁻, might occur in natural^{10,11} as well as in synthetic carbonated apatites.¹²⁻¹⁵

In the present study, the constitution of the NCAp's prepared in our previous study³ by the hydrolysis of CaHPO₄, was determined after heating at 110, 150, 250, and 400 °C. On the basis of a physical and chemical characterization of the samples, the absolute contribution of the substitution mechanisms responsible for the Na⁺- and CO₃²⁻-incorporation in these apatites was derived.

Experimental Section

Preparation and Heating of NCAp. For the present study the samples used were prepared in a previous investigation.³ These NCAp's were synthesized by the hydrolysis of monetite (CaHPO₄) at 95 °C for 5 h in a Na₂CO₃ solution with a concentration *c*_{nc} ranging from 0.010 to 0.250 M and dried at 25 °C under vacuum. More details on the preparation as well as on the composition of these samples are given

[®] Abstract published in *Advance ACS Abstracts*, November 1, 1994.

- (1) Senior Research Associate of the NFSR (Belgium).
- (2) Driessens, F. C. M.; Verbeeck, R. M. H. *Biomaterials*; CRC Press: Boca Raton, FL, 1990.
- (3) De Maeyer, E. A. P.; Verbeeck, R. M. H.; Naessens, D. E. *Inorg. Chem.* 1993, 32, 5709.
- (4) De Maeyer, E. A. P.; Verbeeck, R. M. H.; Naessens, D. E. *J. Cryst. Growth* 1994, 135, 539.
- (5) LeGeros, R. Z.; Trautz, O. R.; LeGeros, J. P.; Klein, E. *Bull. Soc. Chim. Fr.* 1968, 1712.
- (6) Bonel, G. *Ann. Chim.* 1972, 7, 127.
- (7) Labarthe, J. C.; Bonel, G.; Montel, G. *Ann. Chim.* 1973, 8, 289.
- (8) Vignoles, C.; Bonel, G.; Montel, G. *C. R. Hebd. Séances Acad. Sci., Ser. C* 1975, 280 (6), 361.
- (9) Bonel, G.; Labarthe, J. C.; Vignoles, C. *Coll. Int. CNRS* 1975, 230, 117.

- (10) Holcomb, D. W.; Young, R. A. *Calcif. Tissue Int.* 1980, 31, 189.
- (11) Mayer, I.; Schneider, S.; Sydney-Zax, M.; Deutsch, D. *Calcif. Tissue Int.* 1990, 46, 254.
- (12) Dowker, S. E. P.; Elliott, J. C. *Calcif. Tissue Int.* 1979, 29, 177.
- (13) Vignoles, M.; Bonel, G.; Young, R. A. *Calcif. Tissue Int.* 1987, 40, 64.
- (14) Vignoles, M.; Bonel, G.; Holcomb, D. W.; Young, R. A. *Calcif. Tissue Int.* 1988, 43, 33.
- (15) De Maeyer, E. A. P. Ph.D. Thesis, University of Ghent, Ghent, Belgium, 1992.

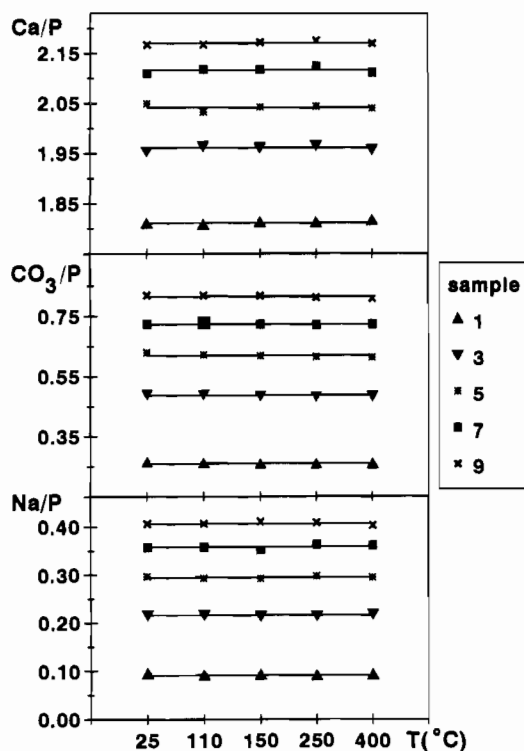


Figure 1. Molar ratios of the NCAp's prepared by the hydrolysis of monetite as a function of drying temperature for some representative samples.

elsewhere.³ The NCAp's were consecutively dried at a constant temperature of 110, 150, 250, and 400 °C in air. At each temperature the drying process was continued until a constant weight was obtained which usually took about 2 weeks.

Chemical Analysis. The calcium content of the precipitates was determined by a complexometric titration with ethylenediaminetetraacetic acid¹⁶ and the phosphorus content spectrophotometrically as the orthophosphate by using a slight modification of the method of Brabson *et al.*¹⁷ The sodium content of the samples was determined by atomic absorption spectrophotometry and the carbonate content coulometrically.³ The relative uncertainties on the amount Ca, P, CO₃ and Na analyzed were determined as 0.2, 0.2, 2 and 2%, respectively.

Physical Analysis. X-ray powder diffraction patterns of the samples were recorded by step-scanning using a microprocessor-controlled diffractometer system (Philips PW 1830). Ni-filtered copper K α radiation was used with an automatic divergence slit PW1836 and a graphite monochromator. The dimensions *a* and *c* of the hexagonal unit cell of the apatites were calculated from the position of the most intense and sharp reflections (usually *n* > 19) using a least squares refinement program. The experimental errors of *a* and *c* were estimated as 0.0006 and 0.0002 nm, respectively. IR-spectra of the samples dispersed in CsBr tablets were recorded using a Mattson Galaxy 6030 Fourier transform infrared spectrophotometer. The density of the samples was measured with a helium micropycnometer of Quantachrome Corp. with an accuracy of 0.2%. Scanning electron microscopy (Jeol, JSM-6400) was carried out on some samples after they were gold-coated.

Results

Chemical Composition. The relative chemical composition of the NCAp's expressed as the molar ratios of the constituent ions, is given for some representative samples in Figure 1 as a function of the drying temperature. The figure shows that the

Table 1. ANOVA on the Basis of a Two-Factor Design of the Logarithmic Transforms of the CO₃/Ca Ratio of NCAp's Prepared by the Hydrolysis of Monetite and dried at 25, 110, 150, 250, and 400 °C (Source of Variation; Degrees of Freedom *df*; Sum of Squares *SS*; Mean Square *MS*; *F*-Test Criterion *F* and Corresponding Significance Level *p*)

source	df	SS	MS	<i>F</i>	<i>p</i>
<i>T</i>	4	1.042 × 10 ⁻³	2.605 × 10 ⁻⁴	0.65	0.631
<i>c_{nc}</i>	9	2.583	2.870 × 10 ⁻¹	717.5	<<0.001
<i>T</i> × <i>c_{nc}</i>	36	2.522 × 10 ⁻⁴	7.004 × 10 ⁻⁶	0.02	>>0.999

Table 2. ANOVA on the Basis of a Two-Factor Design of the Logarithmic Transforms of the CO₃/P Ratio of NCAp's Prepared by the Hydrolysis of Monetite and dried at 25, 110, 150, 250, and 400 °C (Source of Variation; Degrees of Freedom *df*; Sum of Squares *SS*; Mean Square *MS*; *F*-Test Criterion *F* and Corresponding Significance Level *p*)

source	df	SS	MS	<i>F</i>	<i>p</i>
<i>T</i>	4	9.879 × 10 ⁻⁴	2.470 × 10 ⁻⁴	0.62	0.654
<i>c_{nc}</i>	9	3.706	4.118 × 10 ⁻⁴	1029	<<0.001
<i>T</i> × <i>c_{nc}</i>	36	4.064 × 10 ⁻⁴	1.129 × 10 ⁻⁵	0.03	>>0.999

relative composition apparently is independent of the drying temperature within experimental error. This is corroborated by an analysis of variance (ANOVA)¹⁸ of the molar ratios on the basis of a two-factor design (i.e. the temperature *T* and the concentration *c_{nc}* of the Na₂CO₃ solution). The results of the ANOVA for the logarithmic transforms of the CO₃/Ca and CO₃/P ratios are summarized respectively in Tables 1 and 2.

Table 1 shows that the variation of the CO₃/Ca ratio is not the result of the drying process. This indicates that no carbonate is lost upon heating the samples to 400 °C. Moreover, there is no significant interaction between the drying temperature and *c_{nc}*. However, the concentration of Na₂CO₃ most significantly affects the CO₃/Ca ratio of the solid as could be expected.

A similar conclusion can be drawn when the ANOVA results for the CO₃/P ratios in Table 2 are considered. According to Table 2, the CO₃/P ratio of the solids is drastically affected by the concentration of Na₂CO₃. However, CO₃/P is independent of the drying temperature and no significant interaction between the drying temperature and *c_{nc}* occurs. Since no carbonate is lost upon heating, this result confirms that no phosphorus was present as HPO₄²⁻.^{3,4} Indeed, upon heating at temperatures < 400 °C, HPO₄²⁻ ions would be pyrolyzed to P₂O₇⁴⁻ ions.¹⁹⁻²¹ Consequently, the orthophosphate content which is experimentally determined would be reduced and the CO₃/P ratio would increase.

The total mass balance $\Sigma\%$ of the samples at the respective drying temperatures is represented in Figure 2 as a function of the molar Ca/P ratio of the solid. Since the phosphorus in the samples is present as PO₄³⁻ [see also ref 3], the total mass balance can be calculated from the equation

$$\Sigma\% = \% \text{Ca} + \frac{\% \text{P} \cdot M_{\text{PO}_4}}{M_{\text{P}}} + \% \text{CO}_3 + \% \text{Na} + \% \text{OH} \quad (1)$$

with *M_X* the atomic or ionic mass of X. The hydroxide content % OH was calculated on the basis of the electroneutrality condition and the experimentally determined contents of Ca, P, Na and CO₃. The errors of % OH and $\Sigma\%$ were estimated by means of error propagation theory. Figure 2 shows that for

(16) Flaschka, H. A.; Barnard, A. J. Titrations with EDTA and related compounds. Wilson, C. L., Wilson, D. W., Eds.; In *Comprehensive analytical chemistry*, Vol. I^B; Elsevier Publ. Co.: Amsterdam, 1960.
 (17) Brabson, J. A.; Dunn, R. L.; Epps, E. A.; Hoffman, W. M.; Jacobs, K. D. *J. Assoc. Off. Agric. Chem.* 1958, 41, 517.

(18) Meloun, M.; Miliký, J.; Forina, M. *Chemometrics for analytical chemistry*, Vol. I; Ellis Horwood Ltd.: New York, 1992; p 197.
 (19) Berry, E. E. *Bull. Soc. Chim. Fr.* 1968, 1765.
 (20) Berry, E. E. *J. Inorg. Nucl. Chem.* 1967, 29, 317.
 (21) Young, R. A.; Holcomb, D. W. *Calcif. Tissue Int.* 1984, 36, 60.

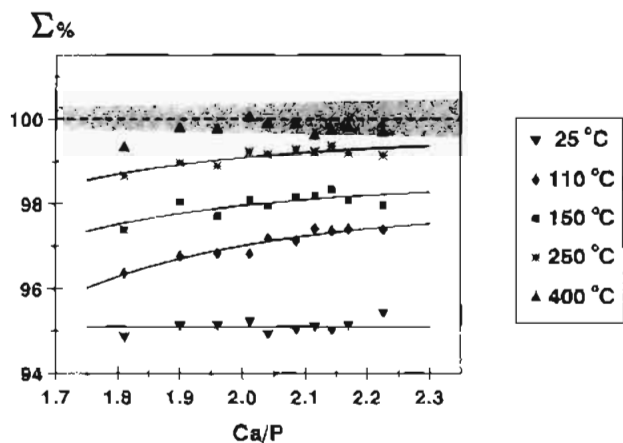


Figure 2. Total mass balance $\Sigma\%$ of NCAp's as a function of their molar Ca/P ratio at different drying temperatures. The 95% confidence limits on $\Sigma\% = 100$ are indicated by the grey zone.

Table 3. Chemical Composition (Weight %) and Total Mass Balance $\Sigma\%$ of the NCAp's Obtained by Hydrolysis of CaHPO_4 in Solutions Containing c_{nc} M Na_2CO_3 after Drying at 400 °C with Calculated Uncertainties in Parentheses

sample	c_{nc}	Ca	P	CO_3	Na	OH	$\Sigma\%$
1	0.010	38.29	16.29	8.12	1.11	1.88 (0.13)	99.35 (0.17)
2	0.025	37.85	15.38	11.3	1.79	1.71 (0.15)	99.80 (0.19)
3	0.050	37.22	14.69	13.8	2.38	1.33 (0.18)	99.77 (0.20)
4	0.075	37.05	14.22	15.3	2.74	1.37 (0.20)	100.06 (0.22)
5	0.100	36.67	13.89	16.5	3.03	1.13 (0.21)	99.92 (0.23)
6	0.125	36.49	13.51	17.5	3.27	1.21 (0.22)	99.90 (0.24)
7	0.150	36.10	13.21	18.5	3.54	1.01 (0.23)	99.65 (0.25)
8	0.175	36.02	13.00	19.1	3.71	1.07 (0.24)	99.76 (0.25)
9	0.200	35.91	12.79	20.0	3.82	0.90 (0.25)	99.84 (0.26)
10	0.250	35.64	12.38	21.0	4.11	0.99 (0.26)	99.70 (0.27)

a given sample the total mass balance increases with increasing drying temperature. This indicates that more water is lost by the samples as the temperature is increased. With only one exception (i.e. for sample 1 with the lowest carbonate or Ca/P ratio), $\Sigma\%$ reaches 100% at 400 °C within experimental error. Attempts to eliminate the residual water of sample 1 by drying at higher temperatures failed as a drastic loss of CO_3^{2-} occurs at temperatures above 400 °C. A most striking observation is that according to Figure 2 the total mass balance apparently depends on the composition of the NCAp at a given temperature in the range $110 \leq T$ (°C) ≤ 250 . Moreover, this dependency of $\Sigma\%$ on Ca/P becomes less pronounced with increasing drying temperature.

The chemical compositions of the NCAp's dried at 400 °C are summarized in Table 3 as a function of the Na_2CO_3 concentration during the hydrolysis. From Table 3 it is seen that, as the Na_2CO_3 concentration in the solution increases, the CO_3 and Na content of the solid increases, whereas the Ca, P, and OH content decreases.

Physical Analysis. The X-ray diffraction patterns of the samples dried at higher temperatures do not differ from those of the samples dried at 25 °C. The peaks in the patterns are sharp and well resolved, and can all be attributed to the hexagonal crystal form of hydroxyapatite (ASTM Powder Diffraction File No. 9-432). Extraneous peaks attributable to phases other than apatite are not introduced by the heating process. Consequently, the crystallinity and purity of the NCAp's are not influenced by the heating process. Figure 3 gives the lattice parameters a and c of the samples dried at 25 and 400 °C as a function of the carbonate content (wt %) determined after drying at 400 °C. It can be seen that a as well as c tend to be systematically smaller for the samples dried at 400 °C. However, a regression analysis shows that for the

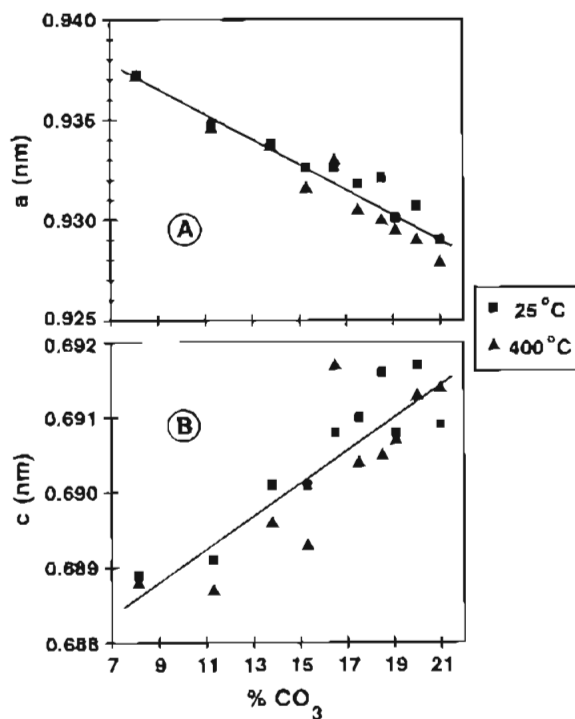


Figure 3. Lattice parameters a (nm) (A) and c (nm) (B) of the NCAp's after drying at 25 °C (■) and 400 °C (▲) as a function of carbonate content (wt %) after drying at 400 °C.

samples dried at 400 °C, the lattice parameters vary according to

$$a_{400} = (0.9429 \pm 0.0021) - (6.9 \pm 1.3) \times 10^{-4} [\% \text{CO}_3]_{400} \quad (2)$$

$$c_{400} = (0.6866 \pm 0.0019) + (2.3 \pm 1.2) \times 10^{-4} [\% \text{CO}_3]_{400} \quad (3)$$

whereas for the samples dried at 25 °C the following relationships hold:³

$$a_{25} = (0.9417 \pm 0.0018) - (5.7 \pm 1.1) \times 10^{-4} [\% \text{CO}_3]_{400} \quad (4)$$

$$c_{25} = (0.6871 \pm 0.0013) + (2.1 \pm 0.8) \times 10^{-4} [\% \text{CO}_3]_{400} \quad (5)$$

The uncertainties of the regression parameters in eqs 2–5 correspond to the 95% confidence level and the subscripts refer to the drying temperature. Equations 2–5 show that heating the samples up to 400 °C does not significantly affect the lattice dimensions of the NCAp's. Consequently, the variation of the lattice parameters of NCAp's as a function of the carbonate content can be estimated on the basis of the pooled data resulting in eqs 6 and 7. Eqs 6 and 7 are represented in Figure 3 by the

$$a = (0.9423 \pm 0.0015) - (6.3 \pm 0.9) \times 10^{-4} [\% \text{CO}_3]_{400} \quad (6)$$

$$c = (0.6868 \pm 0.0010) + (2.2 \pm 0.6) \times 10^{-4} [\% \text{CO}_3]_{400} \quad (7)$$

full lines. The decrease of a and the increase of c with increasing CO_3 content is typical for B-type CO_3^{2-} incorporation.^{2,3}

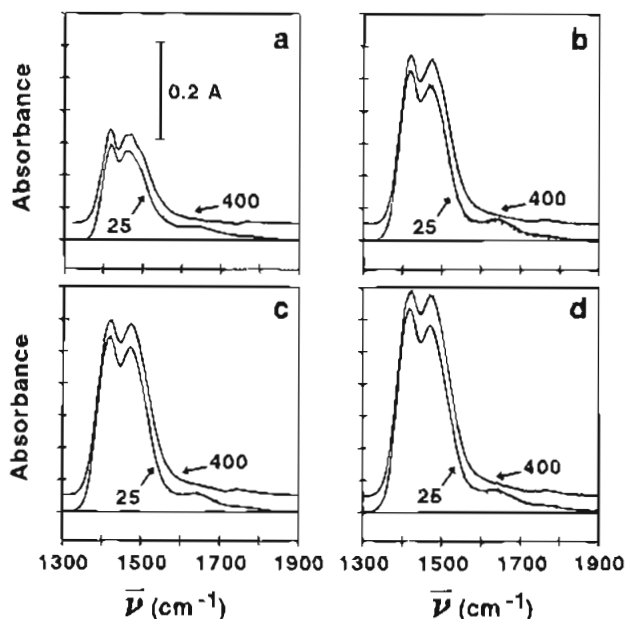


Figure 4. IR spectra of sample 1 (a), 3 (b), 6 (c) and 10 (d) between 1300 and 1900 cm^{-1} (absorbance A versus wavenumber $\bar{\nu}$ (cm^{-1})) after drying at 25 and 400 °C.

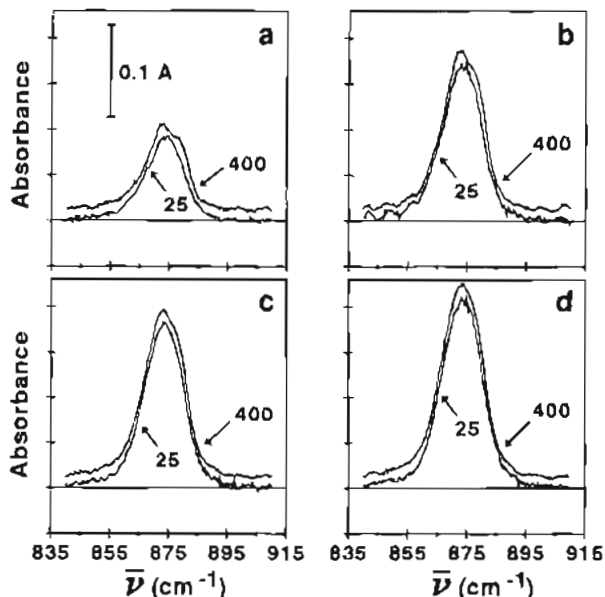


Figure 5. IR spectra of samples 1 (a), 3 (b), 6 (c) and 10 (d) between 835 and 915 cm^{-1} (absorbance A versus wavenumber $\bar{\nu}$ (cm^{-1})) after drying at 25 and 400 °C.

The IR-spectra of the samples are typical for CO_3^{2-} -containing apatite with typical absorptions in the ranges 960–1100 and 570–610 cm^{-1} arising from PO_4^{3-} , around 3572 and 633 cm^{-1} due to the stretching vibration and libration of OH^- ions and around 873 and 1415 as well as between 1464 and 1480 cm^{-1} caused by the vibrations of CO_3^{2-} on PO_4^{3-} lattice sites.²³ Upon heating to 400 °C the spectra of the NCAp samples are not drastically changed. With increasing drying temperature the broad absorption bands of H_2O around 3400 and 1635 cm^{-1} observed after drying at 25 °C³ gradually decrease and are completely eliminated after drying at 400 °C. This trend can be seen from Figure 4 which gives a detailed view of the 1300–1900 cm^{-1} region for some representative samples dried at 25 and 400 °C.

The disappearance of the broad water band around 3400 cm^{-1} results in an enhanced detectability of the 3572 cm^{-1} OH^- stretching vibration. The intensity of this absorption decreases

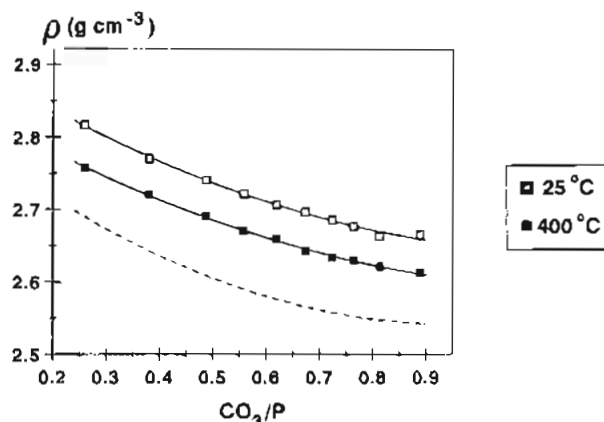


Figure 6. Density ρ (g cm^{-3}) of NCAp's dried at 25 and 400 °C, as a function of their molar CO_3/P ratio. The broken line represents ρ^* as calculated from eq 10.

with increasing carbonate content of the samples. The profiles of the PO_4^{3-} absorptions are not affected by the heating process and absorptions arising from HPO_4^{2-} or $\text{P}_2\text{O}_7^{4-}$ ions^{19,20} could not be detected respectively before or after heating. However, after heating at 400 °C the CO_3^{2-} absorption bands exhibit some details which become less pronounced with increasing carbonate content. This can be illustrated with Figures 4 and 5. The latter one gives a detailed view of the CO_3^{2-} absorptions in the 835–915 cm^{-1} region. The figures show that shoulders appear around 1500 and 880 cm^{-1} upon heating whose intensity decreases with increasing carbonate content. Moreover, the decrease apparently is more pronounced for the shoulder near 1500 cm^{-1} than for that around 880 cm^{-1} .

The density of the samples after drying at 25 and 400 °C is represented in Figure 6 as a function of the molar CO_3/P ratio of the solid. As the stoichiometry of the apatite is not affected by the drying process (see Figure 1), the mean value was taken for the CO_3/P ratio at the drying temperatures investigated. A weighted regression analysis shows that the density as a function of CO_3/P is represented at the 95% confidence level by the equations

$$\rho_{25} = (2.926 \pm 0.031) - (0.48 \pm 0.11)[\text{CO}_3/\text{P}] + (0.20 \pm 0.10)[\text{CO}_3/\text{P}]^2 \quad (8)$$

$$\rho_{400} = (2.862 \pm 0.014) - (0.443 \pm 0.052)[\text{CO}_3/\text{P}] + (0.181 \pm 0.044)[\text{CO}_3/\text{P}]^2 \quad (9)$$

for the samples dried at 25 and 400 °C, respectively. From eqs 8 and 9 and from Figure 6, it can be seen that the density of the samples decreases with increasing CO_3 content of the samples. Moreover, upon heating at 400 °C the density is significantly reduced which is merely due to a shift of the $(\rho, \text{CO}_3/\text{P})$ -curve toward lower densities without a change in slope or curvature.

Figures 7 and 8 show the SEM pictures of some representative samples after drying at 25 °C. From these figures, it can be seen that the NCAp samples consist of bar- or platelike particles with a magnitude of about 10 μm . This morphology compares to that found by Ishikawa and Eanes²² for hydroxyapatites obtained by the hydrolysis of CaHPO_4 in CO_2 -free aqueous solutions. The particles are composed of aggregated crystallites which are more or less acicular for the less carbonated NCAp's (Figure 7; sample 1) and spherical for the highly carbonated NCAp's (Figure 8; sample 10). The same holds for the samples

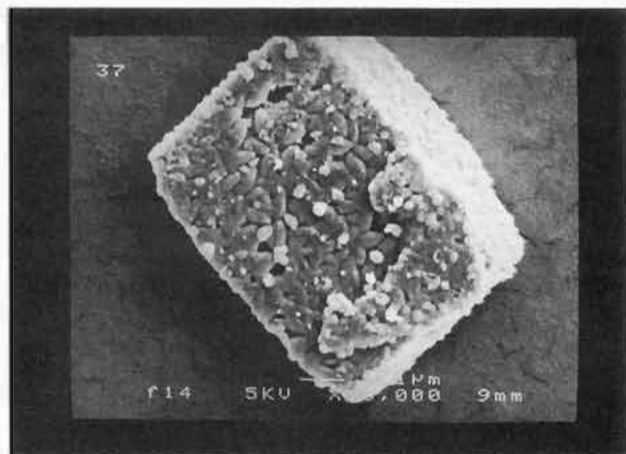


Figure 7. Scanning electron micrograph of sample 1 after drying at 25 °C.

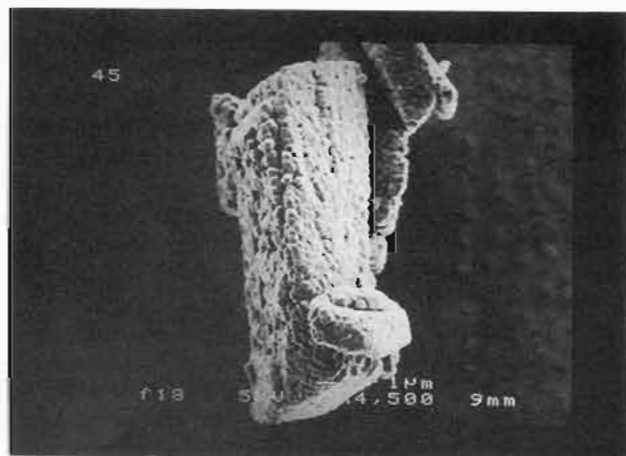


Figure 8. Scanning electron micrograph of sample 10 after drying at 25 °C.

heated up to 400 °C. However, whereas the morphology of sample 10 has not changed upon heating, sample 1 appears to be slightly sintered as its crystallites seem to be melted together at the contact points.

Discussion

To a first approximation, the thermal decomposition between room temperature and ~1000 °C of carbonated apatites and apatitic calcified tissues consists in a loss of water and carbonate. The water from the apatites includes structural as well as nonstructural water. The nonstructural water can be adsorbed on or occluded between the particles. Structural water (lattice water) can be substitutional (water on vacant lattice sites) and/or water involved in solid state reactions (e.g. the pyrolysis of HPO_4^{2-} to pyrophosphate).^{9,23,24}

The dehydration and CO_2 evolution of natural and synthetic apatites have been studied by several investigators. However, the results are not consistent. LeGeros *et al.*²³ investigated the dehydration of natural apatites (human enamel) and synthetic NCAp. They found that adsorbed water could be removed at 200 °C, while the lattice water could be driven out at 400 °C. Davidson and Arends²⁴ establish that the "loosely bound water" of tooth enamel is driven out completely at 150 °C, while the "firmly bound water" is evolved between 150 and 400 °C. Holcomb and Young¹⁰ on the contrary, state that structural water

can still be observed up to 800 °C. The inconsistency of these literature data could be ascribed to the difference in chemical and physical properties of the samples studied, as well as to differences in the experimental procedures used for the study of the heating process.

The carbonate loss of synthetic (N)CAp's is reported to start between 500 to 600 °C.^{13,25} However, some investigators noticed some important constitutional changes even below 500 °C. From 300 °C¹³ or even from 200 °C¹⁴ on, some CO_2 appears to be formed in the crystal lattice of the apatites, which can be observed by an absorption in the IR spectra at 2340 cm^{-1} . This absorption disappears at higher temperatures (~700 °C¹³), indicating a loss of CO_2 . Tooth enamel samples exhibit a carbonate loss at temperatures lower than 200 °C.^{10,11} A CO_2 absorption near 2340 cm^{-1} was observed between 200 and 800 °C. Holcomb and Young¹⁰ found some indications that the loss of part of the B-type CO_3^{2-} is accounted for by the migration to an OH^- lattice site, with CO_2 as an intermediate. The newly formed A-type CO_3^{2-} (i.e. CO_3^{2-} substituting for OH^-) is then driven off at higher temperatures (>800 °C). The results of Mayer *et al.*¹¹ are in line with this mechanism.

The results of the chemical and physical analyses of the present NCAp's show that, with only one exception, heating at 400 °C can remove all the water from the apatites without a loss of carbonate, the formation of CO_2 , or other major constitutional changes. This indicates that the apatites investigated in the present study are much more stable with respect to decarbonation as compared to other synthetic or natural apatites.

As mentioned before, the water of the samples can include structural as well as nonstructural water. The elimination of nonstructural water, with a lower density than apatite, would result in an increase of the density of the sample. The elimination of structural water on the other hand, would result in a decrease of the density. Indeed, in view of the fact that the lattice dimensions do not change significantly upon dehydration, the unit cell volume remains approximately the same whereas the mass of the sample decreases. Since the density decreases with increasing temperature (Figure 6), it can be concluded that the water that has been driven out was, at least partly, structural. In view of the fact that the present NCAp's do not contain HPO_4^{2-} ions,^{3,4} the structural water corresponds to water incorporated on vacant lattice sites of the apatite as suggested by some authors.^{9,23,24} Though statistically not significant, the fact that the *a* and *c* lattice dimensions generally tend to be somewhat lower after heating at 400 °C (see Figure 3) could corroborate the elimination of such structural water upon heating.²³

Some of the water of the NCAp's was nonstructural. This can be shown by calculating the theoretical density of the apatites after drying at 400 °C, ρ^* , on the assumption that all the water present after drying at 25 °C was structural, i.e. by using eq 10. In eq 10, the subscripts refer to the drying

$$\rho^* = [\rho]_{25} \frac{[\Sigma\%]_{25}}{[\Sigma\%]_{400}} \quad (10)$$

temperatures. The results of this calculation are represented in Figure 6 by the broken line. The figure shows that the experimental density of the samples after drying at 400 °C is systematically higher than ρ^* . This should be ascribed to the effect of elimination of nonstructural (adsorbed or occluded) water.

(23) LeGeros, R. Z.; Bonel, G.; Legros, R. *Calcif. Tissue Res.* 1978, 26, 111.

(24) Davidson, C. L.; Arends, J. *Caries Res.* 1977, 11, 313.

(25) Legros, R.; Godinot, C.; Torres, L.; Mathieu, J.; Bonel, G. *J. Biol. Buccale* 1982, 10, 3.

Table 4. Unit Cell Composition of NCAp's Obtained by Hydrolysis of CaHPO₄ in Solutions Containing *c*_{nc} M Na₂CO₃ after Drying at 400 °C Calculated by Means of Eqs 11–16 with Values Corrected for the Presence of Nonstructural Water in Parentheses

sample	<i>c</i> _{nc}	<i>n</i> _{Ca}	<i>n</i> _P	<i>n</i> _{CO₃}	<i>n</i> _{Na}	<i>n</i> _{OH}	<i>n</i> _{V^{Ca}}	<i>n</i> _{V^{OH}}	<i>O</i> _P
1	0.010	8.31 ± 0.03 (8.67 ± 0.04)	4.58 ± 0.01 (4.77 ± 0.02)	1.18 ± 0.02 (1.23 ± 0.02)	0.420 ± 0.008 (0.438 ± 0.009)	0.96 ± 0.07 (1.00 ± 0.07)	1.27 ± 0.03 (0.89 ± 0.04)	1.04 ± 0.07 (1.00 ± 0.07)	5.75 ± 0.03 (6.00)
2	0.025	8.06 ± 0.02 (8.27 ± 0.05)	4.24 ± 0.01 (4.35 ± 0.02)	1.61 ± 0.03 (1.65 ± 0.02)	0.66 ± 0.01 (0.68 ± 0.01)	0.86 ± 0.08 (0.88 ± 0.08)	1.28 ± 0.03 (1.05 ± 0.06)	1.14 ± 0.08 (1.12 ± 0.08)	5.85 ± 0.04 (6.00)
3	0.050	7.84 ± 0.02	4.00 ± 0.01	1.94 ± 0.04	0.87 ± 0.02	0.66 ± 0.09	1.29 ± 0.03	1.34 ± 0.09	5.94 ± 0.04
4	0.075	7.70 ± 0.02	3.83 ± 0.01	2.12 ± 0.04	0.99 ± 0.02	0.67 ± 0.10	1.31 ± 0.03	1.33 ± 0.10	5.95 ± 0.04
5	0.100	7.64 ± 0.02	3.74 ± 0.01	2.30 ± 0.05	1.10 ± 0.02	0.55 ± 0.10	1.26 ± 0.03	1.45 ± 0.10	6.04 ± 0.05
6	0.125	7.50 ± 0.02	3.59 ± 0.01	2.40 ± 0.05	1.17 ± 0.02	0.59 ± 0.11	1.33 ± 0.03	1.41 ± 0.11	5.99 ± 0.05
7	0.150	7.39 ± 0.02	3.50 ± 0.01	2.53 ± 0.05	1.26 ± 0.03	0.49 ± 0.11	1.35 ± 0.04	1.51 ± 0.11	6.03 ± 0.05
8	0.175	7.36 ± 0.02	3.44 ± 0.01	2.61 ± 0.05	1.32 ± 0.03	0.52 ± 0.11	1.32 ± 0.04	1.48 ± 0.11	6.04 ± 0.05
9	0.200	7.31 ± 0.02	3.37 ± 0.01	2.72 ± 0.05	1.35 ± 0.03	0.43 ± 0.12	1.34 ± 0.04	1.57 ± 0.12	6.08 ± 0.06
10	0.250	7.21 ± 0.02	3.24 ± 0.01	2.84 ± 0.06	1.45 ± 0.03	0.47 ± 0.12	1.34 ± 0.04	1.53 ± 0.12	6.08 ± 0.06

As can be seen from the SEM pictures (see Figure 7 and 8), water occluded within isolated microvoids is very likely to exist between the aggregated crystallites when the samples are not thoroughly dried, e.g. at 25 °C under vacuum. At each temperature a constant Σ% was reached for a given sample and Σ% increases with increasing CO₃ content at a given temperature (110 ≤ *T* (°C) ≤ 250; see Figure 2). An explanation for this peculiar behavior could be that with increasing temperature the isolated microvoids are gradually forced open thereby enabling an increased loss of occluded water. The lower the carbonate content, the better the stacking of or the higher the entanglement between the crystallite aggregates. This is supported by the difference in morphology as illustrated by Figures 7 and 8. Moreover, sintering was observed for the low-carbonate NCAp's after heating at 400 °C. Consequently, the low-carbonate apatites could exhibit a greater mechanical resistance to an opening of the microvoids. The resistance apparently is so great for the low-carbonate NCAp's that a complete elimination of water cannot be achieved for sample 1 by heating at 400 °C.

As the relative composition as well as the unit cell dimensions of the NCAp's apparently are not affected after drying at 400 °C, the unit cell content of the precipitates dried at 25 °C equals within experimental error the unit cell content of the samples dried at 400 °C with the exception of some structural water. As the total mass balance of the samples dried at 400 °C generally equals 100% within experimental error, their unit cell content is obtained by calculating the number of each ion *X* per unit cell, *n*_{*X*}, from the results of their chemical (Table 3) and physical (Figures 3 and 6) analyses using eqs 11–13. In

$$V_{\text{cell}} = \frac{\sqrt{3}}{2} a^2 c \quad (11)$$

$$M = \rho_{400} V_{\text{cell}} \quad (12)$$

$$n_X = \frac{(\% X) M N_A}{100 M_X} \quad (13)$$

eqs 11–13 *V*_{cell} and *M* represent the unit cell volume and the molar mass of the apatite respectively, % *X* the content of *X*, and *N*_A Avogadro's constant. The results of these calculations are summarized in Table 4. *n*_{V^{Ca}} and *n*_{V^{OH}} respectively give the number of vacancies on Ca²⁺ and OH⁻ lattice sites and were calculated according to

$$n_{V^{\text{Ca}}} = 10 - n_{\text{Ca}} - n_{\text{Na}} \quad (14)$$

$$n_{V^{\text{OH}}} = 2 - n_{\text{OH}} \quad (15)$$

The errors in Table 4 were estimated by means of error propagation theory. The last column of Table 4 shows that the

sum of the number of phosphate and carbonate ions per unit cell, i.e.

$$O_P = n_P + n_{\text{CO}_3} \quad (16)$$

equals 6 within experimental error for samples 3–10 with a mean value of *O*_P = (6.02 ± 0.02). This indicates that CO₃²⁻ substitutes for PO₄³⁻ on a 1:1 basis in these apatites, which agrees with the fundamental substitution mechanisms for B-type CO₃²⁻ derived in ref 26. The mechanism proposed by McConnell *et al.*^{27,28} and Nelson *et al.*,²⁹ according to which 4 CO₃²⁻ ions replace 3 PO₄³⁻ ions, can indeed be excluded on this basis. Moreover, the presence of A-type CO₃²⁻ is once more ruled out. The dispersion of *O*_P found in the present study is much smaller than the one reported by other investigators for samples prepared under heterogeneous precipitation conditions.^{7,9} However, for samples 1 and 2 a significant deviation of *O*_P from 6 is observed (see Table 4). This can be related to the fact that these samples still contain a small amount of nonstructural water, as was shown by the significant deviation of Σ% from 100% for sample 1 (Figure 2, Table 3) and by the acicular morphology combined with a sintering of the crystallites for the low-carbonate apatites (Figure 7 and 8). The latter could result in a permanent fixation of some isolated microvoids, thus increasing the apparent volume occupied by the crystallites. The presence of such nonstructural water and/or permanent microvoids results in an underestimation of the unit cell content of apatite.³

On the basis of the observation that for samples 3–10, CO₃²⁻ substitutes for PO₄³⁻ on a 1:1 basis, one can assume that this also applies for samples 1 and 2. The real number of each ion per unit cell for samples 1 and 2 can then be obtained by multiplying *n*_{*X*} by the factor 6/*O*_P. The results of this correction with the corresponding errors as estimated using error propagation theory, are given in brackets in Table 4.

From Table 4 it is seen that *n*_{Ca} decreases when *n*_{CO₃} increases. A weighted regression analysis shows that the relationship between these quantities at the 95% confidence level conforms to eq 17.

$$n_{\text{Ca}} = (9.75 \pm 0.27) - (0.93 \pm 0.12)n_{\text{CO}_3} \quad (17)$$

From the intercept of eq 17 it can be seen that within experimental error, a carbonate free apatite (*n*_{CO₃} = 0) contains 10 Ca²⁺ ions per unit cell. The slope of eq 17 then suggests

(26) De Maeyer, E. A. P.; Verbeeck, R. M. H. *Bull. Soc. Chim. Belg.* 1993, 102 (9), 601.

(27) McConnell, D. *J. Dent. Res.* 1952, 31, 53.

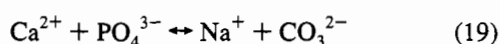
(28) McConnell, D. *Apatite*; Springer Verlag, Vienna, 1973.

(29) Nelson, D. G. A.; Featherstone, J. D. B. *Calcif. Tissue Int.* 1982, 34, S69.

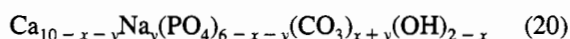
Table 5. Contributions of Mechanisms I (x), III (y), and IV (z) per Unit Cell of NCAp Calculated by Means of Eqs 22, 23, and 26

sample	x	y	z
1	0.89 ± 0.04	0.34 ± 0.03	0.10 ± 0.03
2	1.05 ± 0.06	0.60 ± 0.04	0.08 ± 0.03
3	1.29 ± 0.03	0.65 ± 0.05	0.22 ± 0.05
4	1.31 ± 0.03	0.81 ± 0.05	0.18 ± 0.05
5	1.26 ± 0.03	1.04 ± 0.06	0.06 ± 0.05
6	1.33 ± 0.03	1.07 ± 0.06	0.10 ± 0.06
7	1.35 ± 0.04	1.18 ± 0.06	0.08 ± 0.06
8	1.32 ± 0.04	1.29 ± 0.07	0.03 ± 0.06
9	1.34 ± 0.04	1.38 ± 0.07	-0.03 ± 0.06
10	1.34 ± 0.04	1.50 ± 0.07	-0.05 ± 0.06

that the substitution of a PO_4^{3-} ion by a CO_3^{2-} ion is accompanied by the loss of approximately one Ca^{2+} ion. This indicates that from the four fundamental mechanisms for B-type CO_3^{2-} incorporation,²⁶ only two should be considered as represented by eqs 18 and 19. The mechanisms represented



by eqs 18 and 19 are further referred to as mechanisms I and III, respectively, and result in a stoichiometry of NCAp as given by eq 20, where x and y represent their respective contribution



per unit cell to the stoichiometry. A weighted regression analysis at the 95% confidence level of the data in Table 4 shows that the number of Ca^{2+} ions in the unit cell decreases with increasing n_{Na} according to eq 21. From this observation and

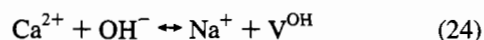
$$n_{\text{Ca}} = (9.69 \pm 0.35) - (2.61 \pm 0.72)n_{\text{Na}} + (0.63 \pm 0.36)n_{\text{Na}}^2 \quad (21)$$

from the fact that $n_{\text{CO}_3} > n_{\text{Na}}$ and $n_{\text{V}^{\text{Ca}}} \approx n_{\text{V}^{\text{OH}}}$ (Table 4), it becomes clear that both mechanisms I and III mainly determine the stoichiometry of the NCAp's obtained in the present study. This substantiates in a direct way the conclusions of our previous study.³ The contributions x and y of the mechanisms I and III to the stoichiometry can be calculated according to eqs 22 and 23. The results are summarized in Table 5 together with the

$$x = n_{\text{V}^{\text{Ca}}} \quad (22)$$

$$y = n_{\text{CO}_3} - x \quad (23)$$

errors estimated by means of error propagation theory. A comparison of Tables 4 and 5 shows that $n_{\text{Na}} \geq y$ indicating that for some samples a Na^+ incorporation has also occurred according to eq 24.²⁶ The mechanism represented by eq 24 is



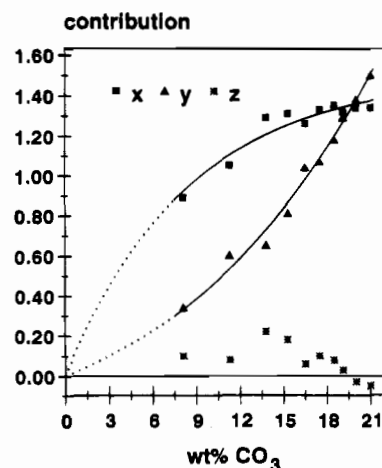
further denoted as mechanism IV and results in a stoichiometry of NCAp as given by eq 25 where z gives its contribution per



unit cell. The z contribution can be calculated from eq 26 and

$$z = n_{\text{Na}} - y \quad (26)$$

is given in the last column of Table 5. Indications for the occurrence of an individual Na^+ incorporation according to

**Figure 9.** Contribution per unit cell of mechanisms I (x), III (y), and IV (z) to the stoichiometry of the NCAp's as a function of their carbonate content.

mechanism IV were also found in our previous study³ by the slight displacement of the line describing the relationship between the CO_3/P and the Ca/P molar ratio of the samples from the line which describes theoretically this relationship on the basis of mechanisms I and III (ref 3; Figure 7). Moreover, the z contribution also accounts for the small negative deviation from 10 of the intercept of the line describing n_{Ca} as a function of n_{CO_3} (eq 17).

In Figure 9 the contributions of the mechanisms are plotted as a function of the carbonate content of the NCAp's. From Figure 9, it can be seen that the x contribution from the individual CO_3^{2-} incorporation according to mechanism I initially increases with increasing CO_3 content. However, at higher CO_3 contents, the variation of x apparently levels off. Mechanism I seems to reach its maximum contribution for $x \approx 1.35$. Supplementary CO_3^{2-} incorporation should then take place in combination with Na^+ incorporation according to mechanism III. The y contribution of this mechanism continuously increases with increasing CO_3^{2-} incorporation (see Figure 9). On the other hand, the z contribution from the individual Na^+ incorporation according to mechanism IV hardly changes as a function of the carbonate content and hence with c_{nc} .

Although the relative chemical composition and the lattice dimensions of the present NCAp's are not affected within experimental error by the heating process, the IR analysis indicates that some minor constitutional changes might be induced. The appearance of the shoulders around 880 and 1500 cm^{-1} after heating at 400 °C (see Figure 4 and 5) could indicate that a migration of CO_3^{2-} from a B-type site to an A-type site (CO_3^{2-} substituting for OH^-) has occurred, as was found for the thermal decomposition of tooth enamel.^{10,11} However, the presence of intermediate CO_2 entrapped in the crystal lattice could not be observed by an IR absorption at 2340 cm^{-1} in the present study. Moreover, Vignoles *et al.* noticed for synthetic NH_4^+ -containing carbonated apatites heated at 400 °C that the relative intensity of this absorption increases with increasing CO_3 content of the sample.^{13,14} In this respect the fact that, for the present samples, the presumed A-type absorptions can only be observed at a low carbonate content remains peculiar. A possible explanation could be that the increase of mechanism III with increasing carbonate content (eq 19) gradually blocks the migration of CO_3^{2-} , e.g. by a concomitant decrease of the lattice dimensions.

Another explanation of the appearance of the absorptions at ~ 880 and ~ 1500 cm^{-1} is that they reflect a stabilization of the CO_3^{2-} ions in the lattice upon heating. This stabilization is

then manifested by a splitting of the CO_3^{2-} absorption bands reflecting the different substitution mechanisms for the CO_3^{2-} incorporation. The fact that the visibility of the absorptions near 880 and 1500 cm^{-1} decreases with increasing CO_3 content would suggest that they can be ascribed to CO_3^{2-} associated with mechanism I. Indeed, the relative contribution of this mechanism as compared to mechanism III, giving rise to absorptions near 873 and 1470 cm^{-1} , decreases with increasing carbonate content.

Conclusions

On the basis of the exact composition of the unit cell of NCAp's prepared by the hydrolysis of CaHPO_4 , the contributions of the mechanisms responsible for the Na^+ and CO_3^{2-} incorporation in the HAp lattice were derived. The contributions of the two predominant mechanisms, i.e. [I: $\text{Ca}^{2+} + \text{PO}_4^{3-} + \text{OH}^- \leftrightarrow \text{V}^{\text{Ca}} + \text{CO}_3^{2-} + \text{V}^{\text{OH}}$] and [III: $\text{Ca}^{2+} + \text{PO}_4^{3-} \leftrightarrow \text{Na}^+ + \text{CO}_3^{2-}$], increase with increasing Na_2CO_3 concentration in solution. However, the contribution of the individual CO_3^{2-}

incorporation (mechanism I) per unit cell apparently reaches a constant level of ~ 1.35 . This could indicate that a limit is reached of the solid solubility of the component corresponding to this mechanism in HAp. Apart from these two mechanisms, there is a small contribution of an individual Na^+ incorporation [IV: $\text{Ca}^{2+} + \text{OH}^- \leftrightarrow \text{Na}^+ + \text{V}^{\text{OH}}$]. As was shown in ref 3 and as can be seen from Figure 9 and Table 5, the relative contribution of these mechanisms to the stoichiometry of NCAp changes with carbonate content and hence with c_{nc} . However, a partial coupling between them can not be excluded. Such a coupling cannot be inferred on the basis of the present results, since the Na^+ and CO_3^{2-} concentrations in solution are varied simultaneously by using Na_2CO_3 as a reagent. Further experiments, in which the contributions of mechanism I and III are changed independently could elucidate this matter.

Acknowledgment. This work is part of a project supported by the "Executieve van de Vlaamse Gemeenschap-Departement Onderwijs" which is gratefully acknowledged.